

Investigation of domain wall motion in RE-TM magnetic wire towards a current driven memory and logic



Hiroyuki Awano

Toyota Technological Institute, Tempaku, Nagoya 468-8511, Japan

ARTICLE INFO

Article history:

Received 20 June 2014

Received in revised form

29 December 2014

Accepted 31 December 2014

Available online 9 January 2015

Keywords:

Memory and logic

Magnetic wire

Spin logic

TbFeCo

Rare earth transition metal

Amorphous

ferrimagnetism

Critical current density

Low magnetization

Domain wall velocity

AND

OR

NOT

NAND

NOR

Polycarbonate substrate

Si substrate

Nano-imprint

ABSTRACT

Current driven magnetic domain wall (DW) motions of ferri-magnetic TbFeCo wires have been investigated. In the case of a Si substrate, the critical current density (J_c) of DW motion was successfully reduced to 3×10^6 A/cm². Moreover, by using a polycarbonate (PC) substrate with a molding groove of 600 nm width, the J_c was decreased to 6×10^5 A/cm². In order to fabricate a logic in memory, a current driven spin logics (AND, OR, NOT) have been proposed and successfully demonstrated under the condition of low J_c . These results indicate that TbFeCo nanowire is an excellent candidate for next generation power saving memory and logic.

© 2015 The Author. Published by Elsevier B.V. This is an open access article under the CC BY license (<http://creativecommons.org/licenses/by/4.0/>).

1. Introduction

Current driven domain wall (DW) motion has attracted much attention for new applications, such as low-power, high-speed, logic devices. Particularly, long-term preservation of data is possible because it does not have mechanical operation parts. DW displacement by spin polarized current was predicted by Berger [1]. Then, a lot of experimental results with in-plane magnetized FeNi magnetic wires have been reported [2–5]. The critical current density (J_c) of FeNi nanowire required large value of over 1×10^8 A/cm², and the J_c reduction was a big issue. Using FeNi nanowire, racetrack memory has been proposed [6] and demonstrated the accurate operation. Then several experiments have been conducted, J_c value was successfully reduced to 3×10^7 A/cm² by using a perpendicular magnetized Co/Ni nanowire [7–9]. As a reason of J_c reduction, it was considered that DW motion of Co/Ni nanowire is due to only intrinsic pinning effect [10,11]. It was very attractive to explain every experimental result

by theoretical analysis. Therefore, the wall pinning force of Co/Ni nanowire has a very low value, it is considered that Co/Ni nanowire is not suitable for external data storage. Because external storage material such as HDD and computer tape requires large DW pinning force to save data with high reliability. However, it was considered that J_c is proportional to DW pinning force [12]; it seems that coexistence of low J_c and large DW pinning force is difficult.

On the other hand, J_c of perpendicular magnetized TbFeCo has been reported [13–18] as 3×10^6 A/cm² which is lower than that of Co/Ni. The DW pinning force was over 1 kOe and it can be easily controlled by Tb composition. It seems that coexistence of low J_c and large DW pinning force is possible in the TbFeCo nanowire. Moreover, in the TbFeCo nanowire, there are high density and relatively uniform pinning sites. Therefore, arbitrary shape domain can be recorded. In the case of Co/Ni nanowire, it requires a lot of artificially fabricated notches at the wire edge to keep position of recorded domains [7]. From these results, it seems that rare earth

transition metal alloy such as TbFeCo is an attractive material for magnetic wire memory.

By the way, memory and logic are placed separately in the current computer, the memory and logic are connected by a data bus. Therefore, operation speed is rate-limiting in the communication speed between memory and logic. If memory and logic are prepared in the same area and directly connected each other, the operation speed would be improved. However, in the most spin logic reports [19–22], FeNi in-plane magnetized nanowires were used and most logics were operated by a rotational magnetic field from outside of the device. Therefore, current driven spin logic has been proposed. In this article, drastic J_c reduction of TbFeCo nanowire with PC substrate is reported, and low current driven AND, OR, and NOT operations with TbFeCo nanowire are presented.

2. Experimental procedure

The 0.3–1.5 μm -wide and 100- μm -length wire patterns were fabricated using electron beam lithography for a lift-off process as shown in Fig. 1(a). In this case, it is considered that the lift off process damages the magnetic film. Therefore, a new fabrication method with nanoimprint technique is proposed in Fig. 1(b). This method is similar to the optical disk fabrication and the substrate cost is very low compared with that of the Si substrate. When a magnetic film is deposited onto the grooved PC substrate, magnetic nanowire can be prepared without any damage. The 20-nm-thick $\text{Tb}_{26}\text{Fe}_{66.8}\text{Co}_{7.2}$ film was directly grown on SiO_2/Si substrate by RF magnetron sputtering. A Pt film with a thickness of 2 nm was subsequently capped on the film. The ultimate vacuum was less than 2×10^{-8} Torr and Ar sputtering gas pressure of 1 mTorr was kept during grown films. Ti/Al contacts were defined by optical lithography on top of each TbFeCo electrode. A scanning electron microscopy (SEM) image of the fabricated sample is shown in Fig. 2. The magnetic properties of the films and wires were measured using an alternating gradient force magnetometer

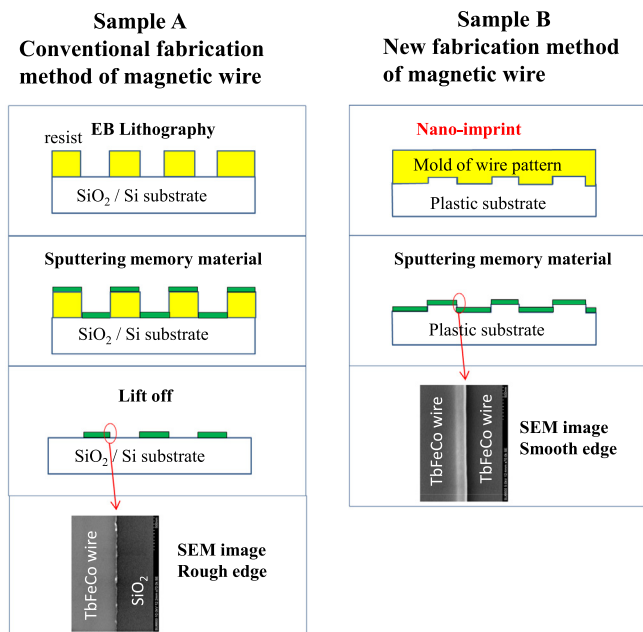


Fig. 1. Sample A: general fabrication process of magnetic nanowire. Sample B: proposed new fabrication process of magnetic nanowire. The feature is similar to the optical disk fabrication process. Therefore, the new fabrication process is attractive for low cost magnetic wire preparation and low J_c sample.

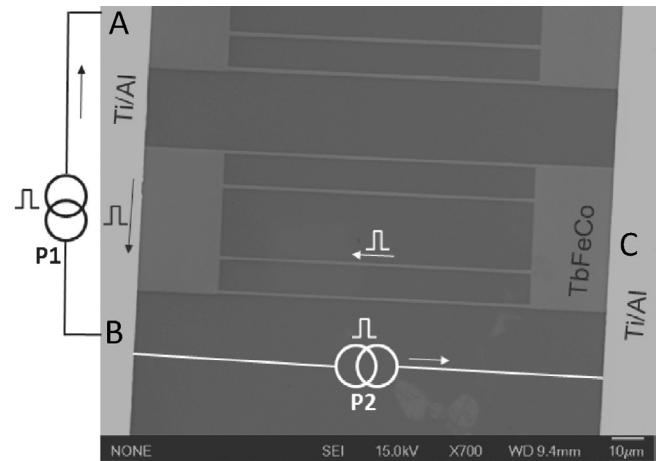


Fig. 2. SEM image of the Sample A set up for magnetic spin memory.

(AGFM) and anomalous Hall voltage measurement. When a domain wall motion of the sample is observed, magnetically initialize process is performed to the sample using larger external magnetic field over the coercive force (H_c). Then, the magnetic DWs were created in the wires by using an Oersted field which is generated by current flow from the electrode A to B in Fig. 3. The motion of DWs was driven by current flow from the electrode C to B. Pulse voltage duration was 100 ns. The DWs dynamics in the wires were directly observed using polar Kerr microscopy as shown in Fig. 4. Hysteresis loop measurement on the films using AGFM (data not shown) confirmed that the films had a good perpendicular magnetic anisotropy with a saturation magnetization of $M_s = 110 \text{ emu/cm}^3$.

3. Results and discussion

3.1. Very low current driven DW motion in TbFeCo wire

Using the sample of Fig. 2, current driven DW motions in

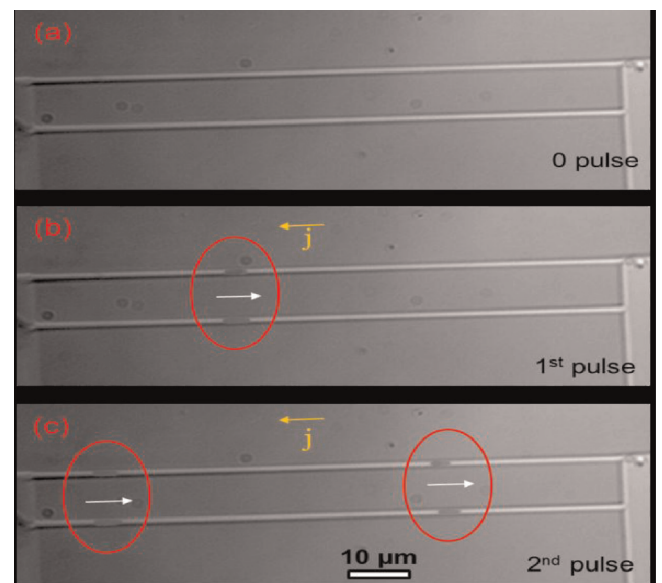


Fig. 3. Polar Kerr optical microscope image of TbFeCo magnetic nanowires on SiO_2/Si substrate. (a) After initialize process, (b) in each magnetic wire, one domain is recorded, then 1st pulse current is applied, each domain is displaced to the right hand side. (c) 2nd Domain is recorded at the left hand side, then injected 2nd pulse current drive both the 1st and 2nd recorded domains.

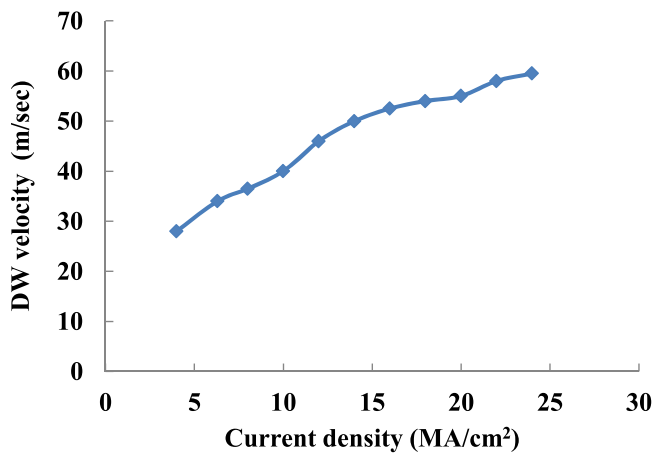


Fig. 4. Current density dependence of DW velocity in the TbFeCo wire.

TbFeCo wire were observed with Polar Kerr optical microscope. The observation results are shown in Fig. 3. The reason of utilizing two TbFeCo wires is to confirm the possibility of parallel data processing used by high-speed data transmission. After initialization of the TbFeCo was performed, there is no domain as shown in Fig. 3(a). Next, one domain is recorded on the left hand side of the TbFeCo wire, then one pulse current is applied to the wire from the electrode C to B. The recorded domain is displaced to the right hand side as shown in Fig. 3(b). The length of the displaced domain length is almost same as initial one. Moreover, one more domain is recorded to the TbFeCo wire, then the recorded 2 domains are shifted to the right hand side by applying 2nd current pulse as shown in Fig. 3(c). Two domain lengths and the interval length between them did not change even when 2nd current pulse is applied. This result indicates that current driven domain wall motion can be used as a memory device. The direction of the domain wall displacement is opposite to that of the current. Therefore, it is considered that the domain wall motion is caused by spin torque transfer effect [23].

Current density dependence of DW velocity is shown in Fig. 4. It indicates the DW motion of the flow regime. The critical current density (J_c) of the domain wall motion in TbFeCo wire was 5×10^6 A/cm². The value is relatively small compared with another magnetic material. The saturation magnetization (M_s) of the TbFeCo is 110 emu/cm³, it is very low compared with another current driven magnetic materials, because TbFeCo is ferri-magnetic material. Fig. 5 shows M_s dependence of J_c in several magnetic nanowires. It shows that J_c is proportional to M_s .

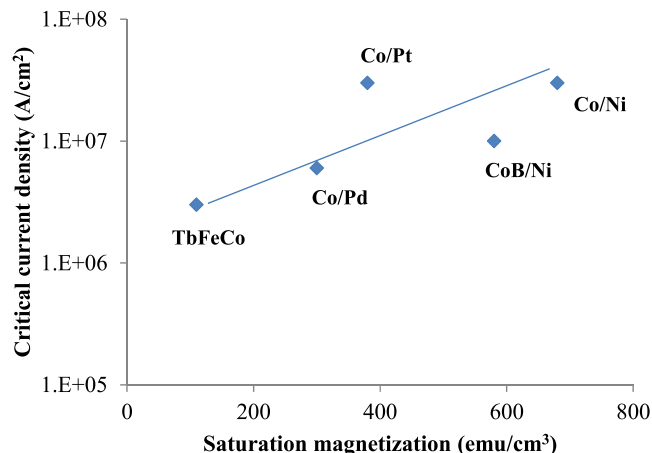


Fig. 5. Saturation magnetization (M_s) dependence of critical current density (J_c) on SiO₂/Si substrate for several kinds of magnetic nanowire.

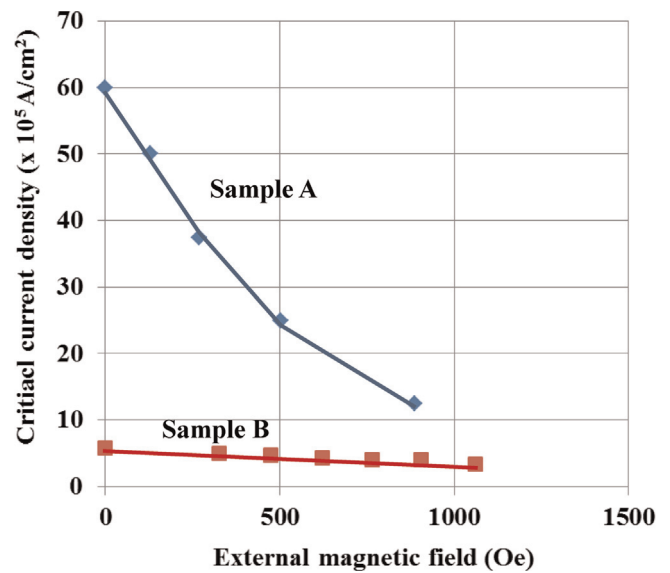


Fig. 6. External magnetic field dependence of J_c for Sample A (Si substrate) and Sample B (PC substrate).

3.2. Future potential estimation of low current driven TbFeCo spin memory with plastic low cost substrate

Thus, a rare-earth transition metal such as TbFeCo is very attractive material for low current driven memory device. For example, TbFeCo was used as a magneto-optical memory and the high durability and reliability of MO products has been demonstrated. The minimum recording domain length in the TbFeCo narrow track was around 40 nm. Also, narrow track pitch for the current driven spin memory can be produced with electron beam lithography technique. In the case of wire memory fabrication of Sample A in Fig. 1(a), both substrate cost and process cost are very high. However, in the case of Sample B in Fig. 1(b), both costs can be drastically reduced. Fig. 6 shows external magnetic field dependence of J_c for Sample A and B. In the case of the sample B with grooved PC substrate, J_c can be reduced to 6×10^5 A/cm². This result is also very attractive for spin memory. It seems that extrinsic pinning effect of PC substrate is much smaller than that of Si substrate. In the case of nanoimprint, thinner PC substrate also can be used. Moreover, nano-imprint can be pressed for both surfaces of the PC substrate. This means both side can be used for spin memory. In one side surface area of PC substrate (65 mm in width \times 90 mm in length) which is similar area of SSD and 2.5" HDD form factor, data capacity of 40 nm bit and track pitch can be calculated as 450 GB. If both side spin memory with thinner PC substrate of 0.05 mm thickness can be adopted in the form factor, the data capacity would become to 100 TB. This is very attractive value. Thus, nano-imprint magnetic nanowire memory system should be investigated.

3.3. Proposal of low current driven spin logic

If memory and logic devices are designed with smart arrangement in a circuit, problem of interconnection delay can be reduced, it is very attractive for higher performance. Therefore, current driven spin memory and logic (AND, OR, NOT) should be proposed. If these 3 kinds of logic operation can be demonstrated, NAND, NOR, XOR could be also realized. Here, current driven AND, OR and NOT demonstrations with the same operating mechanism due to spin torque transfer effect are discussed. The operating mechanism of AND, OR, NOT are shown in Figs. 7–9, respectively.

In Fig. 7 current driven AND logic, 3 types of INPUT (1, 1), (1, 0),

Current driven AND LOGIC operations

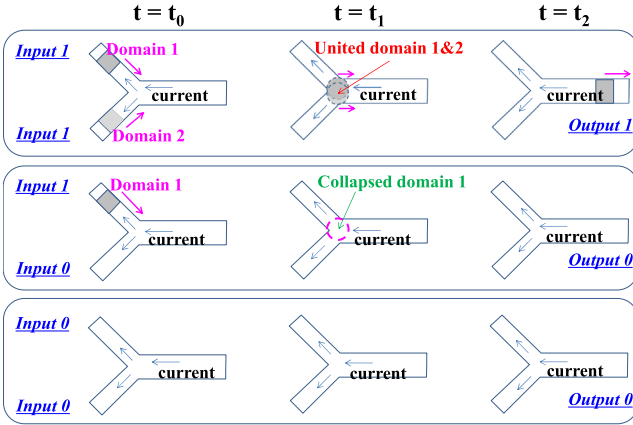


Fig. 7. Schematic figure of current driven AND type spin logic. Upper one is corresponding to the INPUT (1, 1), middle one INPUT (1,0), Lower one INPUT (0, 0).

Current driven OR LOGIC operations

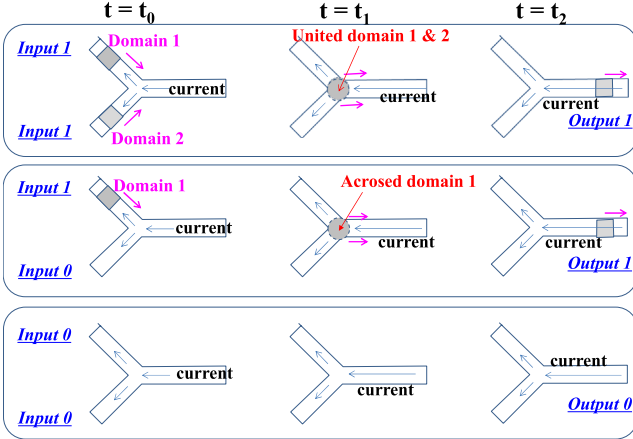


Fig. 8. Schematic figure of current driven OR type spin logic. Upper one is corresponding to the INPUT (1, 1), middle one INPUT (1,0), Lower one INPUT (0, 0).

Current driven NAND LOGIC with NOT GATE

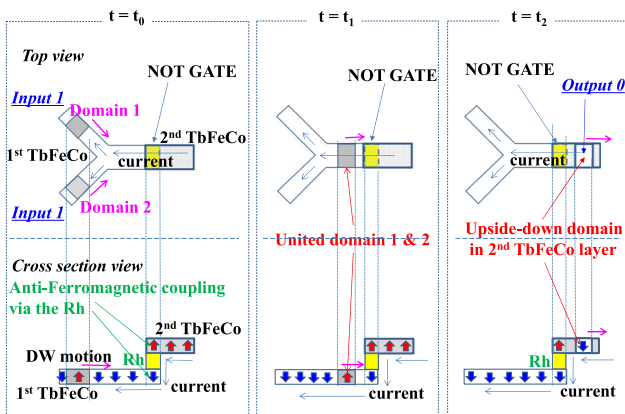


Fig. 9. Schematic figure of current driven NAND and NOT GATE type spin logic. Upper one is corresponding to the NAND process, lower one is corresponding to the NOT GATE.

(0, 0) are shown. For example, in the case of input (1, 1) at $t=t_0$, one domain is recorded on the each input port. When a current is applied from the output port to the input port, both recorded

domains in each input port are displaced to the confluence point. Then two domains are united each other at the confluence point ($t=t_1$). Finally, the united domain is thorough out to the output port ($t=t_2$). Thus, the AND logic operating result of input (1, 1) shows output (1).

On the other hand, in the case of input (1, 0), one domain is recorded on the upper input port ($t=t_0$). When current is flow from the right to the left of the Y-shaped sample, the right domain wall of the domain 1 gets trapped at the junction node, and as the left domain wall of the domain 1 moves toward the right, both domain walls are annihilated along with domain 1 ($t=t_1$). Therefore, output signal shows zero ($t=t_2$). The opposite input case of (0, 1) is also the same result as input (1, 0). It is clear that AND operating result of input (0, 0) is output (0).

In the same way, OR operation can be performed as shown in Fig. 8. The input (1, 1) operation is as same as that of the AND spin logic. On the other hand, in the case of the input (1, 0) case, the output signal should be (1). Therefore, the width of output port should be narrow because the right domain wall of the domain 1 do not be trapped at the junction node ($t=t_1$). In this case, the domain 1 can be flow out to the output port ($t=t_2$).

Finally, the schematic model of NOT function is shown in Fig. 9. Please look at the top view ($t=t_0$) of the NOT GATE and the cross section view. The layer stack structure is substrate/1st TbFeCo/Rh/2nd TbFeCo. In this case, spin direction in the 1st TbFeCo layer is opposite to that of the 2nd TbFeCo layer. This phenomena can be applied to the NOT function. In the figure upper area, current drive NAND logic circuit is indicated and the one part of the output port area works as a NOT GATE. In the figure lower part, a cross section image is represented. The NOT GATE area is composed of 3 layers. Both lower and upper layers are TbFeCo and the intermediate layer is Rh.

Fig. 10 shows Rh layer thickness dependence of remanent polar Kerr rotation angle. Total thickness of the 3 layers is less than 20 nm. The laser penetration depth into the film is about 100 nm. Therefore, the Kerr rotation signal involves magnetic properties of both TbFeCo layers. When the Rh layer is zero, both TbFeCo layers are coupled ferro-magnetically, therefore, the remanent Kerr rotation value is large.

However, when the Rh layer thickness is 0.4 nm, both TbFeCo layers are coupled ferri-magnetically, the remanent Kerr rotation shows very low because magnetization direction of the upper TbFeCo is opposite to that of lower TbFeCo layer. Here, to obtain a

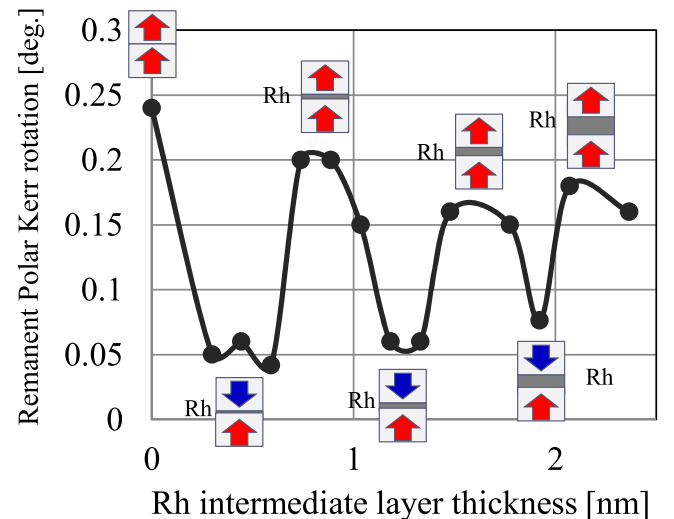


Fig. 10. Rh layer thickness dependence of remanent polar Kerr rotation angle in TbFeCo/Rh/TbFeCo multilayers. When Rh thickness is 0.4 nm, both TbFeCo layers coupled anti ferro-magnetically.

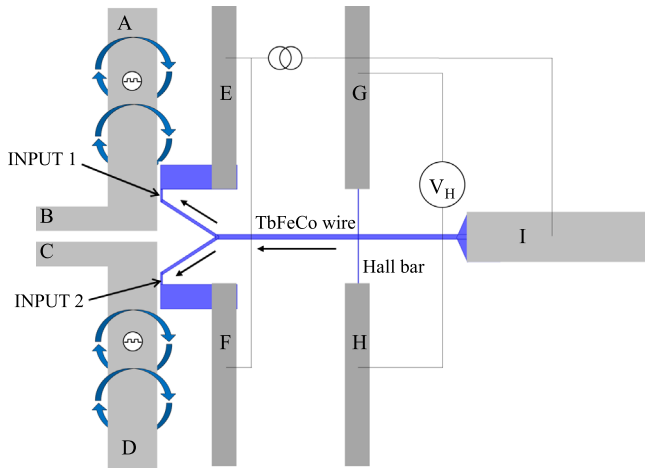


Fig. 11. Schematic figure of current driven AND type spin logic.

strong ferri-magnetic coupling in both TbFeCo layers, Rh layer of 0.4 nm in thickness is used for the NOT GATE sample. When the recorded domain is displaced to the right hand side by current flow as shown in Fig. 11 cross section view of the NOT GATE, the domain at the NOT GATE is copied to the upper TbFeCo layer. In the case, the copied magnetization can be reversed to that of the original domain, because of Rh thickness of 0.4 nm. Thus, the NOT function can be confirmed.

Fig. 11 is an image of current driven AND circuit. When current is applied between the electrode A and B, a domain at the INPUT 1 area of TbFeCo wire can be generated. In the same way, at the INPUT 2 area, a domain recording can be done. When current is applied from electrode I to E and F, the recorded domains at INPUT 1 and 2 area can be displaced to output area. The output signal can be reproduced by detecting anomalous Hall effect between the electrode G and H. The SEM image of AND spin logic experimental setup is shown in Fig. 12. Here, Input 1 and 2 signals are produced at the same time by applying Oersted field current from the electrode B to A. In the case of INPUT (1, 1) operation, If domain wall velocity at the INPUT 1 area is faster than 2 times compared with that of INPUT 2 area, it is difficult to become one output domain at the confluence point. In this case, there is no OUTPUT signal for any INPUT signals.

In order to confirm the current driven AND operation, AND demonstration circuit was prepared as shown in Fig. 13. Here, to simplify the experiment, simple electrode A to B is fabricated. Therefore, it is impossible to create domain corresponding to the INPUT (1, 0). However, In the case of INPUT (1, 1), when the current is applied from the electrode I to E, only one domain at the INPUT

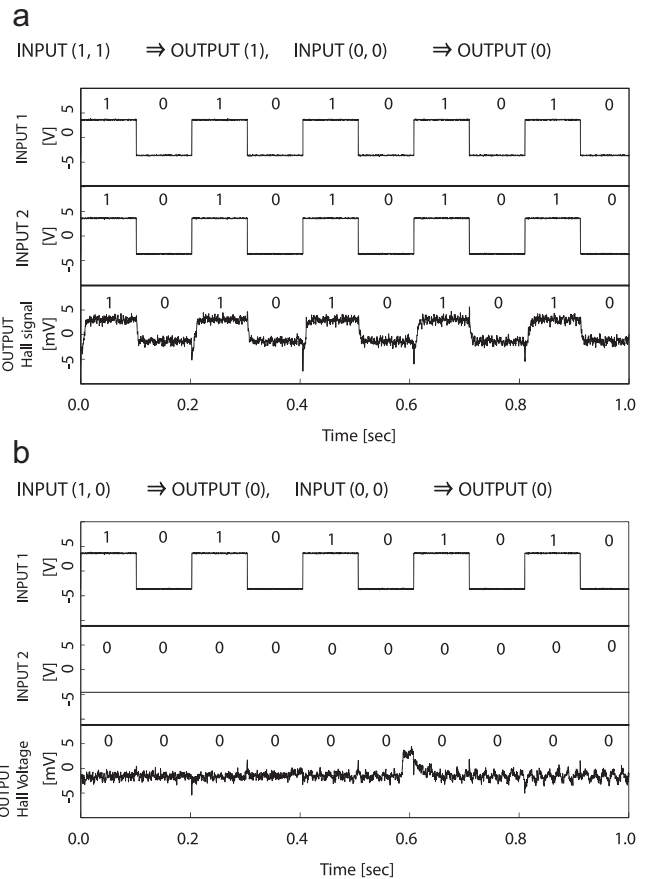


Fig. 13. Experimental result of current driven AND spin logic. (a) When INPUT signal is (1, 1), the operated OUTPUT result is (1). In case of INPUT (0, 0), the OUTPUT result is (0). (b) When INPUT signal is (1, 0), the operated OUTPUT result is (0).

1 area is displaced to the confluence point and collapsed.

Thus, the OUTPUT signal of the INPUT (1, 0) can be confirmed. The experimental result of the current driven AND circuit is shown in Fig. 13(a) INPUT (1, 1) and (0, 0), and (b) (1, 0), and (0, 0). In the case of Fig. 13(a), the upper one and middle one are corresponding to the signals of INPUT 1 and 2, the lower one is corresponding to the OUTPUT signal of Hall voltage. From those figures, it is found that the current driven AND circuit works exactly. In the case of OR circuit, it is more easy, because a domain collapse condition of INPUT (1, 0) at the confluence point can be easily fabricated. Thus, current driven DW memory and logic would be realized.

4. Conclusion

Current driven DW motions in TbFeCo magnetic nanowire were investigated. A critical current density (J_c) of TbFeCo which is prepared with lift off process and the substrate is Si was about 4×10^6 A/cm². It is considered that lower saturation magnetization (M_s) of the ferri-magnetic TbFeCo causes the decrease J_c . On the other hand, J_c of TbFeCo nanowire without any chemical process on PC substrate was 6×10^5 A/cm². This value is quite small compare to that of another magnetic nanowire. It is considered that in the Sample B preparation process named as nano-imprint method, extrinsic pinning sites can be reduced compared with that of the Sample A process named as etching method.

In order to realize current driven memory and logic, new spin logic of AND, OR, NOT have been proposed. These experimental

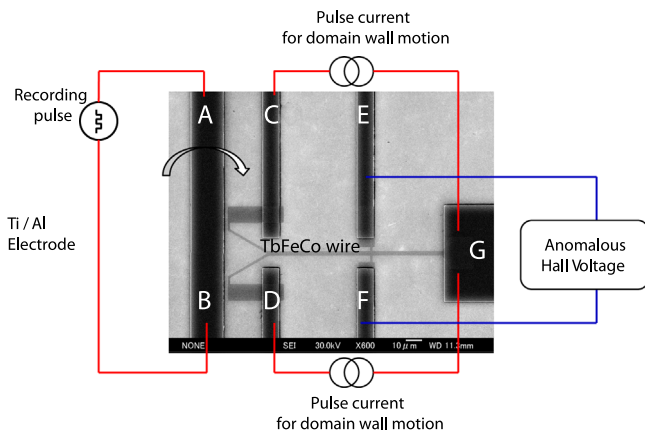


Fig. 12. SEM image of AND sample on SiO₂/Si substrate and experimental setup.

circuits were made and demonstrated. In these spin logic circuit, J_c was 1×10^6 A/cm². Thus, current driven spin memory and logic is very attractive for future memory and logic devices.

Acknowledgments

This work was performed by postdoctoral fellow Duc The Ngo and students Toma Kanehira, Jun Miyamoto, Masahiro Nomura of Toyota Technological Institute. This work was financially supported by the Ministry of Education, Culture, Sports, Science, and Technology, Japan – Supported Program for Strategic Research Foundation at Private University (2009–2013) and KAKENHI No. 24656219 (2012–2014) and No. 24360126 (2012–2015), No. 26630137 (2014–2016).

References

- [1] L. Berger, *Phys. Rev. B* 54 (1996) 9353–9358.
- [2] A. Yamaguchi, T. Ono, S. Nasu, K. Miyake, K. Mibu, T. Shinjo, *Phys. Rev. Lett.* 92 (2004) 077205.
- [3] M. Klaui, C.A.F. Vaz, J.A.C. Bland, W. Wernsdorfer, G. Faini, E. Cambril, L. Heyderman, F. Nolting, U. Rudiger, *Phys. Rev. Lett.* 94 (2005) 106601.
- [4] L. Thomas, M. Hayashi, X. Jiang, R. Moriya, C. Rettner, S.S.P. Parkin, *Nature* 443 (2006) 197.
- [5] L. Thomas, R. Moriya, C. Rettner, S.S.P. Parkin, *Science* 330 (2010) 1810.
- [6] S.S.P. Parkin, M. Hayashi, L. Thomas, *Magnetic domain-wall racetrack memory*, *Science* 320 (2008) 190–194.
- [7] T. Koyama, G. Yamada, H. Taniigawa, S. Kasai, N. Oshima, S. Fukami, N. Ishiwata, Y. Nakatani, T. Ono, *Appl. Phys. Express* 1 (2008) 101303.
- [8] H. Tanigawa, T. Koyama, G. Yamada, D. Chiba, S. Kasai, S. Fukami, T. Suzuki, N. Oshima, N. Ishiwata, Y. Nakatani, T. Ono, *Appl. Phys. Express* 2 (2009) 053002.
- [9] S. Fukami, Y. Nakatani, T. Suzuki, K. Nagahara, N. Oshima, N. Ishiwata, *Appl. Phys. Lett.* 95 (2009) 232504.
- [10] T. Koyama, et al., *Nat. Matter* 10 (2011) 194.
- [11] T. Koyama, K. Ueda, K.-J. Kim, Y. Yoshimura, D. Chiba, K. Yamada, J.-P. Jamet, A. Moughin, A. Thiavill, S. Mizukami, S. Fukami, N. Ishiwata, Y. Nakatani, H. Kohno, K. Kobayashi, T. Ono, *Nat. Nanotech.* 151 (2012) 1.
- [12] D. Ravelosona, D. Lacour, J.A. Katine, B.D. Terris, C. Chappert, *Phys. Rev. Lett.* 95 (2005) 117203.
- [13] S. Li, H. Nakamura, T. Kanazawa, X. Liu, A. Morisako, *IEEE. Trans. Mag.* 46 (2010) 1695.
- [14] D.-T. Ngo, K. Ikeda, H. Awano, *Appl. Phys. Express* 4 (2011) 093002.
- [15] D.-T. Ngo, K. Ikeda, H. Awano, *J. Appl. Phys.* 111 (2012) 083921.
- [16] D. Bang, H. Awano, *Appl. Phys. Express* 5 (2012) 125201.
- [17] D. Bang, H. Awano, *IEEE. Trans. Mag.* 49 (2013) 4390.
- [18] D. Bang, H. Awano, *Jpn. J. Appl. Phys.* 52 (2013) 123001.
- [19] D.A. Allwood, G. Xiong, C.C. Faulkner, D. Atkinson, D. Petit, R.P. Cowburn, *Science* 309 (2005) 1688.
- [20] H. Nomura, R. Nakatani, *Appl. Phys. Exp.* 4 (2011) 013004.
- [21] N. Ohshima, H. Numata, S. Fukami, K. Nagahara, T. Suzuki, N. Ishiwata, K. Fukumoto, T. Kinoshita, T. Ono, *J. Appl. Phys.* 107 (2010) 103912.
- [22] Y. Nakashima, K. Nagai, T. Tanaka, K. Matsuyama, *Appl. Phys. Lett.* 92 (2008) 022505.
- [23] J.C. Slonczewski, *Current-driven excitation of magnetic multilayers*, *J. Magn. Mater.* 159 (1996) L1–L7.